Polish Journal of Veterinary Sciences Vol. 22, No. 2 (2019), 263–270

DOI 10.24425/pjvs.2019.127095

Original article

Influence of simvastatin on hepatocytes – histopathological and immunohistochemical study

M. Mikiewicz, I. Otrocka-Domagała, K. Paździor-Czapula

Department of Pathological Anatomy, Faculty of Veterinary Medicine,
University of Warmia and Mazury in Olsztyn, Oczapowskiego 13, 10-718 Olsztyn, Poland

Abstract

The present study was undertaken to highlight the influence of simvastatin administration on hepatocyte morphology, proliferation, and apoptosis. The study included 48 gilts aged 3 months (weighing ca. 30 kg) divided into groups I (control; n=24) and II, receiving 40 mg/animal simvastatin orally (simavastatin; n=24) for 29 days. The animals were euthanized on days subsequent to the experiment. The livers were sampled, fixed, and processed routinely for histopathology, histochemistry, and immunohistochemistry (for proliferating cell nuclear antigen, Bcl-2, and caspase-3). Apoptosis was visualized by terminal deoxynucleotidyl transferase dUTP nick-end labelling (TUNEL). Simvastatin administration caused acute hepatocyte swelling, glycogen depletion, hyperaemia, multifocal hepatocyte proliferation with occasional pseudoacinar formation, connective tissue hyperplasia, eosinophil infiltration, and interface hepatitis. The proliferating cell nuclear antigen index, mean diameter of argyrophilic nucleolar organizer regions, and Bcl-2 immunoexpression were lower compared to control, and mean caspase-3 immunoexpression was higher in group II compared to control. On day 25 and 29 single hepatocytes in the simvastatin-treated group were TUNEL-positive. Simvastatin caused morphological alteration which became more intense over time. The results from the present study suggest that simvastatin treatment may cause glycogen, lipid metabolism and cell membrane permeability distortion, fibrosis, interface hepatitis, reduction in hepatocyte proliferation and transcriptional activity, and enhanced vulnerability to apoptosis. Summing up the results, it can be concluded that simvastatin caused liver damage with similar morphological changes seen in autoimmune-like liver injury, which may indicate that simvastatin may induce autoimmune-like drug induced liver injury.

Key words: statin, hepatotoxicity, Bcl-2, apoptosis, liver, pig

Correspondence to: M. Mikiewicz, e-mail: mateusz.mikiewicz@uwm.edu.pl, tel.: 0048 89 523 32 22

Introduction

Simvastatin (SIM) is one of the statins that is used worldwide in therapy for hypercholesterolaemia. Statins are selective, competitive inhibitors of 3-hydroxy-3--methylglutaryl-coenzyme A (HMG-CoA) reductase, and they effectively reduce cholesterol synthesis and reduce its level in the serum. Additionally, statins can alter the activities of the paraoxonase 1 (PON1) and butyrylcholinesterase (BuChE) hepatic enzymes, which are hypothetically involved in lipid metabolism (Macan et al. 2015). Statins also act as free radical scavengers. The scavenging actions are achieved by Ras-related C3 botulinum toxin substrate 1 (Rac1) and nicotinamide adenine dinucleotide phosphate-oxidase (NADPH oxidase) inhibition via the inhibition of Rac isoprenylation. Additionally, statins can diminish the mRNA expression of NADPH oxidase subunits and reduce NADPH oxidase activity (Lim et al. 2014).

Unfortunately, statin administration can cause adverse effects including myopathies, rhabdomyolysis and hepatotoxicity (Kubota et al. 2004). It is thought that SIM hepatotoxicity is connected to the decrease in mevalonate biosynthesis, which is a precursor of coenzyme Q10 (CoQ10). Treatment with SIM causes a pronounced reduction in mitochondrial CoQ10 levels and a decrease in cellular antioxidant capacity (Tavintharan et al. 2007). The associated toxicity of statin usage is mostly reflected in the elevation of liver transaminases (Kubota et al. 2004), and it has been hypothesized that the hepatic side effects are connected to the asymptomatic elevation in liver aminotransferases (Calderon et al. 2010). The elevation in liver aminotransferases is often observed in the first 12 weeks of SIM administration at dosage strengths of 20-80 mg daily (Armitage 2007, Calderon et al. 2010). Additionally, it has been demonstrated that SIM hepatotoxicity can increase in cases of simultaneous usage of certain drugs, i.e., nefazodone, amlodipine, and ciprofloxacin (Björnsson et al. 2012). Previous studies have revealed that SIM administered alone can also cause hepatotoxicity (Bhardwaj and Chalasani 2007). However, an accurate mechanism underlying the statin-induced hepatotoxicity is unclear and needs further investigation.

Statins have been proven to affect cell migration, proliferation, survival, and apoptosis (Huang et al. 2015). Statins can restrain cell proliferation by inhibiting the mevalonate pathway and interfering with signalling pathways that require prenylated proteins, such as nuclear laminin B, ras proto-oncogene, Rho-related proteins, and the γ-subunit of the heterotrimeric GTP--binding proteins (Corsini et al. 1999). The proapoptotic actions of statins have been confirmed in striated myofibres, cardiac myocytes, vascular smooth muscle cells, and endothelial cells. This action is caused by decreases in the amounts of farnesyl pyrophosphate and geranylgeranyl pyrophosphate due to the inhibition of HMG--CoA reductase (Kubota et al. 2004). Furthermore, statins can activate the apoptotic mitochondrial pathway through decreases in Bcl-2 activity without changes in the levels of the Bax family proteins and increase executioner caspases-3, and -9 and cytochrome c (Kaminsky and Kosenko 2010). In hepatocellular carcinoma cell lines administration of SIM reduced the numbers of cells in the S phase and arrested them in the G0/G1 cell cycle phase due to reduced expression of cyclin-dependent kinases (CDKs) and enhanced p19 and p27 expression, which resulted in apoptosis (Relja et al. 2010). However, the influences of SIM administration on the proliferation and apoptosis of hepatocytes and thus the regenerative capacity of the liver are unknown.

Currently, statins especially SIM, are the first-line drugs for hypercholesterolaemia treatment, therefore absence of broader comparative studies of the effect of SIM on the liver causes a serious gap in knowledge. Due to the poorly known influence of SIM on liver function, it was considered appropriate to undertake this research to establish the changes in liver morphology, proliferation and apoptosis during SIM therapy. It was hypothesized that the administration of SIM could alter liver morphology and proliferation activity and could trigger apoptosis in hepatocytes. The results of this study will provide new information on this drug regarding the benefit-risk assessment of SIM therapy.

Materials and Methods

This study was performed in accordance with the principles for the care and use of animals and was approved by the Local Ethics Committee for Animal Experiments (opinion No. 61/2010/N). The study was performed on 48 clinically healthy female, large Polish--breed pigs aged 3 months and weighing ca. 30 kg. The animals were randomly divided into two separate experimental groups as follows: (1) group I (control) included 24 pigs without treatment, and (2) group II included 24 pigs that received SIM (Simvasterol; Polpharma, Starogard Gdański, Poland) that was administered per os for 29 days at a daily dose of 40 mg/animal (approx. 1 mg/kg). On days 16, 17, 18, 19, 20, 22, 25, and 29 of the SIM administration, three pigs from each group were euthanized by intravenous injection of pentobarbital sodium salt (Morbital; BIOWET, Puławy, Poland).

Directly after euthanasia, each liver was sampled, fixed in 10% buffered formalin, processed routinely for

Table 1. Primary antibodies used with particular methods of antigen retrieval and visualization system.

Primary Antibody	Clone	Dilution	Incubation time	Source	Antigen retrival	Visualization system
PCNA	Monoclonal mouse anti-PCNA, clone PC10	1:200	30min in room temperature	DAKO, Denmark	2x3min* TrisEDTA buffer pH=9	EnVision + System-HRP, Mouse (DAB)[a]
Caspase-3	Rabbit polyclonal to Caspase 3	1:300	30min in room temperature	Abcam, Great Britain	2x3min* citrate buffer pH=6	ImmPRESS Reagent Kit, Universal (DAB)[b]
Bcl-2	Rabbit polyclonal to Bcl-2	1:100	Overnight in 4°C	Novus Biologicals, USA	2x3min* citrate buffer pH=6	ImmPRESS Reagent Kit, Universal (DAB)[b]

* antigen retrieval was conducted in a microwave oven, 650W
[a] Dako, Glostrup, Denmark
[b] Vector, Burlingame, USA

histopathology, embedded in paraffin wax and cut. The sections were stained with Mayer's haematoxylin and eosin (HE) and periodic acid-Schiff (PAS) according to McManus and Van Gieson's staining protocols (Bio-Optica, Milan, Italy). The nucleolar proteins associated with the nucleolar organizing regions (NORs) were stained according to the Ploton method (Ploton et al. 1986). The Feulgen staining method was used to visualize the DNA distribution (Feulgen and Rossenbeck 1924). The sections for immunohistochemistry were mounted on silanized glass slides and subjected to heat-induced antigen retrieval (Table 1). The immunohistochemical examinations were performed using primary antibodies and a visualization system that was established on the immunoperoxidase method using 3,3-diaminobenzidine (DAB) as the chromogen (Table 1). The slides were counterstained with Mayer's haematoxylin. The positive controls were as follows: (1) PCNA in the skin, (2) Bcl-2 in the B-cell lymphoma cells, and (3) caspase-3 in the tonsils were handled with the evaluated slides. As negative controls, the primary antibody was either replaced with mouse IgG2a (DAKO, Glostrup, Denmark) at an appropriate dilution (for PCNA) or omitted (for Bcl-2 or caspase-3). TUNEL staining for apoptosis was performed using the commercially available Trevigen Apoptotic Cell System (TACS) TdT-DAB in Situ Apoptosis Detection Kit (R&D Systems, Minneapolis, MN, USA) according to the manufacturer's instruction. The sections were counterstained with Mayer's haematoxylin. For a negative control, the TdT enzyme was omitted from the labelling reaction mix for one sample. For a positive control, the TACS-nuclease was added to the labelling reaction mix for one sample. A positive reaction was obtained when a brown precipitate in the immunohistochemistry and TUNEL assay was observed.

The AgNORs (black-stained dots in the nuclei) were counted in 100 hepatocytes (HPF, 400x). The mean number of AgNORs per nucleus (mAgNORs) was counted. The AgNOR proliferation index (pAgNORs) was counted as the percentage of hepatocytes with ≥5 AgNORs/nucleus. The diameters of 100 AgNORs/slide were measured, and the mean diameters of the AgNORs were counted. Quantitative analysis of the eosinophils was performed. Next, eosinophils were counted in ten randomly chosen areas of the slide (10 HPFs, 400x), and the mean eosinophil quantity per HPF (400x) was subsequently obtained. For PCNA, quantitative analyses of Bcl-2 and caspase-3 were performed. The positive cells were counted in ten randomly chosen areas of the slide (10/HPF, 400x). The PCNA, Bcl-2 and caspase-3 indexes are presented as the percentages of positive cells. The slides were evaluated by light microscopy (BX52, Olympus, Tokyo, Japan) using the Cell^B (Olympus, Tokyo, Japan) software and scanned using a digital camera (HVF22CL 3CCD, Hitachi, Tokyo, Japan) and the Panoramic Viewer software (3DHISTECH, Budapest, Hungary). For the statistical analyses, the Mann–Whitney U test for unpaired samples was used. The results were considered to be statistically significant when $p \leq 0.05$ and highly significant when $p \leq 0.01$. Spearman rank correlation analyses were used to detect the correlations between the PCNA, mAgNORs, pAgNORs, AgNORs diameters, caspase-3, Bcl-2, and numbers of eosinophils throughout the experiment (r: Spearman's rank correlation coefficient). The statistical analyses were conducted using Statistica 12 software (StatSoft Inc., Tulsa, OK, USA).

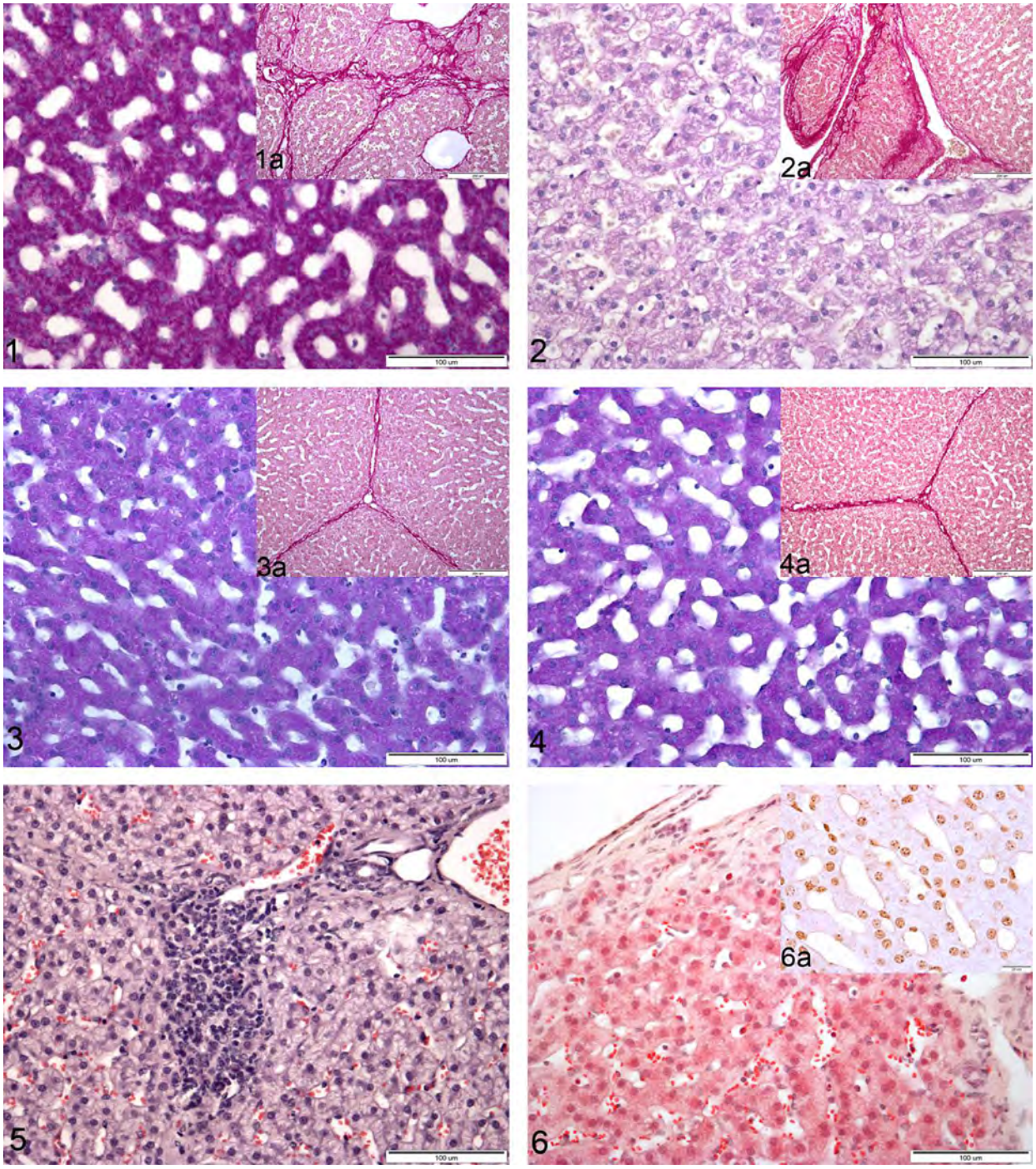

Results

SIM administration caused centrilobular, midzonal, and periportal acute swelling of the hepatocytes and was observed from day 16 until day 29 in all evaluated samples. Additionally, the central veins and sinusoids were dilated and hyperaemic in every liver sample from all animals from the 16th day onward to the 29th day. These changes were absent in the control animals. Furthermore, on day 19, SIM caused randomly distributed macrovesicular fatty degeneration of single hepatocytes, which was not observed in the control group. In the SIM-treated animals, from days 16 to 20, evenly distributed glycogen granules were stored in the cytoplasm of the hepatocytes as confirmed by PAS staining (Fig. 1). However, from day 22, in all sections stained with PAS, the glycogen granules were seldom observed. On the following 25th and 29th days, the glycogen granules were absent as confirmed by PAS staining (Fig. 2). In contrast, in the non-treated animals, the glycogen was evenly distributed in the cytoplasm during the entire experiment, as confirmed with PAS staining (Figs. 3 and 4). In the SIM group, on day 17, two of three pigs exhibited connective tissue hyperplasia (Fig. 1a); furthermore, from day 18 until the end of the experiment, foci of hepatocyte proliferation without central veins and occasionally with

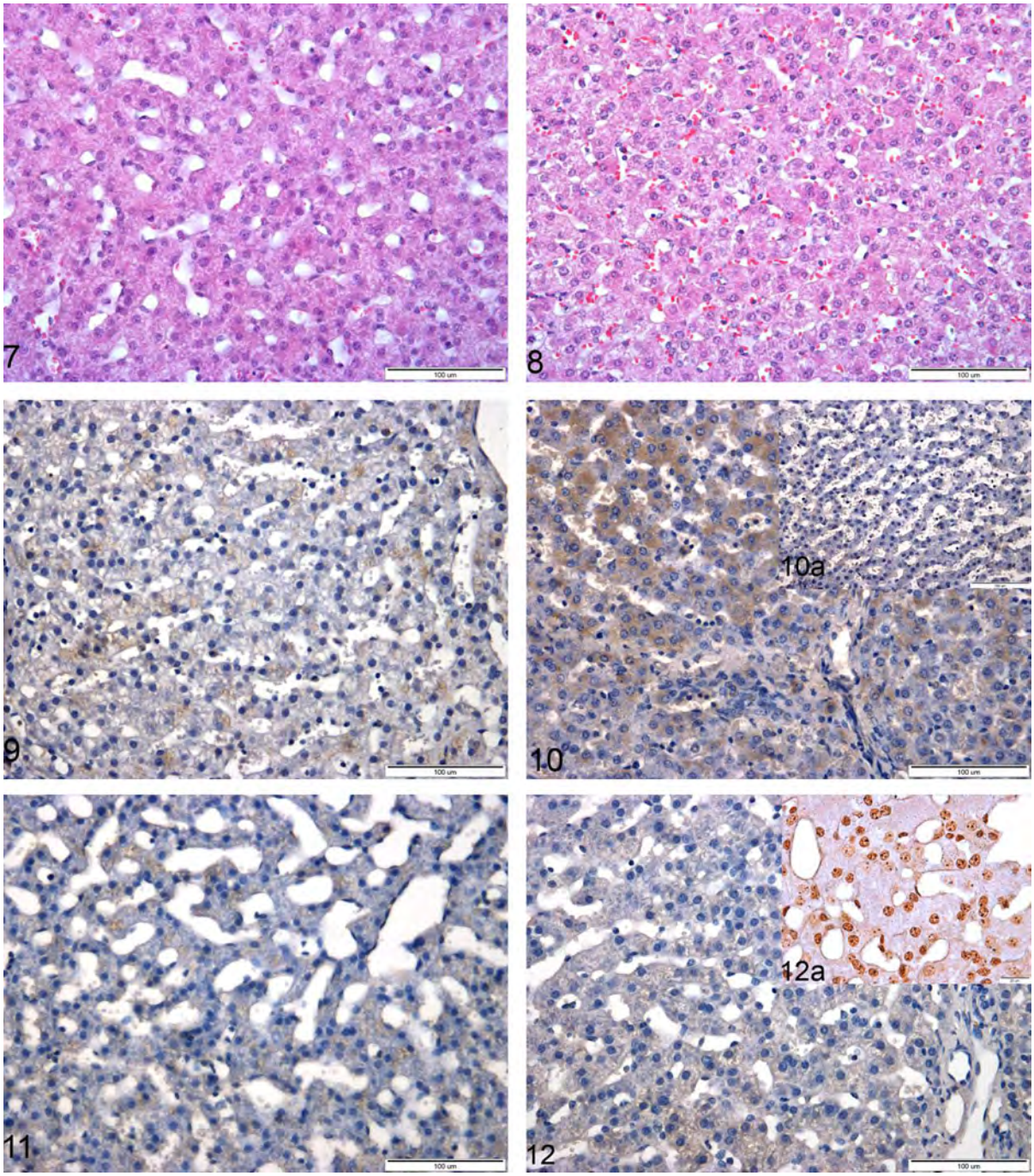

Fig. 1. SIM group, day 16. Small glycogen granules evenly distributed in the hepatocyte's cytoplasm. PAS staining according to McManus, ×400. (1a) SIM group, day 17. Connective tissue hyperplasia between hepatic lobuli. Van Gieson's stain, ×200. Fig. 2. SIM group, day 25. Glycogen granule absence in hepatocytes. PAS staining according to McManus, ×400. (2a) SIM group, day 25. Hyperplastic hepatocyte foci separated by hyperplastic connective tissue. Van Gieson's stain, ×200. Fig. 3. Control group, day 16. Evenly dispersed glycogen in hepatocytes. PAS staining according to McManus, ×400. (3a) Control group, day 16. Normal connective tissue between hepatic lobuli. Van Gieson's stain, ×200. Fig. 4. Control group, day 25. Evenly dispersed glycogen in hepatocytes. PAS staining according to McManus, ×400. (4a) Control group, day 25. Normal connective tissue between hepatic lobuli. Van Gieson's stain, ×200. Fig. 5. SIM group, day 16. Interface hepatitis. HE staining, ×400. Fig. 6. SIM group, day 25. Eosinophil accumulation in sinusoids and near fibrotic area. HE staining, ×400. (6a) SIM group, day 25. Argyrophilic nuclear organizer regions in the nuclei of hepatocytes. Silver staining method according to Ploton, ×1000. Fig. 7. Control group, day 16. Hepatocytes with finely dispersed chromatin and sometimes visible nucleoli. HE staining, ×400. Fig. 8. Control group, day 25. Hepatocytes with finely dispersed chromatin and sometimes visible nucleoli. HE staining, ×400. Fig. 9. SIM group, day 16. Minimal Bcl-2 expression in hepatocytes. Bcl-2 immunolabelling with DAB, ×400. Fig. 10. SIM group, day 19. Bcl-2 expression in periportal hepatocytes. Bcl-2 immunolabelling with DAB, ×400. (10a) SIM group, day 25. Absence of Bcl-2 expression in hepatocytes. Bcl-2 immunolabelling with DAB, ×400. Fig. 11. Control group, day 16. Minimal Bcl-2 cytoplasmic expression in hepatocytes. Bcl-2 immunolabelling with DAB, ×400. Fig. 12. Control group, day 25. Minimal Bcl-2 expression in hepatocytes. Bcl-2 immunolabelling with DAB, ×400. (12a) Control group, day 25. Argyrophilic nuclear organizer regions in the nuclei of hepatocytes. Silver staining method according to Ploton, ×1000.

Table 2. Number of animals exhibiting morphological changes in hepatocytes during simvastatin administration/total number of animals in each day.

	16th day	17th day	18th day	19th day	20th day	22th day	25th day	29th day
Hepatocyte swelling	3/3	3/3	3/3	3/3	3/3	3/3	3/3	3/3
Central vein and sinusoid dilatation	3/3	3/3	3/3	3/3	3/3	3/3	3/3	3/3
Pseudoacinar formation	0/3	0/3	3/3	3/3	3/3	3/3	3/3	3/3
Piecemeal necrosis	3/3	1/3	3/3	3/3	2/3	2/3	2/3	2/3
Connective tissue hyperplasia	0/3	2/3	2/3	3/3	3/3	3/3	3/3	3/3
Hyperplastic hepatocyte foci	0/3	0/3	2/3	3/3	3/3	3/3	3/3	3/3
Eosinophil accumulation	3/3	3/3	3/3	3/3	3/3	3/3	3/3	3/3
Glycogen granules	3/3	3/3	3/3	3/3	3/3	3/3	0/3	0/3

Table 3. PCNA, Bcl-2, and caspase-3 immunoexpression mAgNORs, pAgNORs and eosinophil value in piglet livers (*p≤0.05; **p≤0.01).

Group	PCNA (mean and SD)	Bcl-2 (mean)	Caspase-3 (mean)	mAgNORs (mean and SD)	pAgNORs (mean and SD)	AgNORs diameter (μm; mean and SD)	Eosinophils (mean and SD)
Control	23.84±1.67	5.33	4.71	2.5±0.2	0.06±0.03	1.36±0.16	2.23±1.54
Simvastatin	8.65±7.75**	1.88**	6.17	2.48±0.32	0.05±0.02	1.27±0.14*	18.64±5.92**

pseudoacinar formations without obvious lumina that were separated by hyperplastic connective tissue were noticed (Fig. 2a). In the control group, normal liver architecture with the absence of hyperplastic connective tissue was observed in all examined animals during the entire experiment (Figs. 3a and 4a). On day 16 of the SIM treatment, hepatocytes surrounded by lymphocytes followed by their gradual disappearance were observed in three pigs (interface hepatitis; IH; Fig. 5). On day 17, only one pig exhibited IH, and on days 18 and 19, all three animals developed IH. On days 20 and 22, single areas of IH were observed in two examined samples from two animals. Similar findings were noticed on days 25 and 29 in two examined samples from two animals. In the non-treated animals, IH was absent during the entire experiment. Moreover, during SIM treatment in every examined sample, eosinophil accumulation in the sinusoids, infiltration in the periportal region and fibrotic areas were observed at all analysed time points in the SIM group (Fig. 6). In contrast, eosinophils were seen only occasionally in the control group. The mean value for the eosinophils in the SIM-treated animals was significantly ($p\leq0.01$) increased compared with that in the control group. The detailed morphological changes in the SIM-treated animals are summarized in Table 2. During SIM administration, and similar to the non-treated animals, chromatin was finely dispersed with, occasionally, visible nucleoli (Fig. 7 and 8). Euchromatin predominated over heterochromatin in approximately 90% of the hepatocytes as confirmed by Feulgen staining.

On day 16, minimal cytoplasmic Bcl-2 immunoexpression was observed in single hepatocytes in the SIM-treated animals (Fig. 9). However, on day 19 the immunoexpression was limited to the hepatocytes located in the periportal area or near the connective tissue surrounding the hepatocyte proliferation foci (Fig. 10). From day 25, the Bcl-2 immunoexpression was absent after SIM treatment (Fig. 10a). In contrast, in the non-treated animals, Bcl-2 immunoexpression during the entire experiment was randomly distributed (Figs. 11 and 12). The mean Bcl-2 value during the entire experiment was significantly ($p\leq0.01$) decreased in the SIM-treated animals compared with the control group. Furthermore, significant ($r=-0.47$; $p\leq0.05$) reductions in Bcl-2 immunoexpression were noticed across all of the analysed time points during SIM therapy. This correlation was absent in the control group. In the SIM-treated animals, caspase-3 cytoplasmic immunoexpression was weak to moderate (particularly in the centrilobular hepatocytes from days 19 to 29) during the whole experiment. In contrast, in the non-treated animals, evenly distributed caspase-3 cytoplasmic immunoexpression was weak during the whole experiment. The TUNEL method produced negative results in the SIM group; however, similar to the control group on days 25 and 29, single hepatocytes in all samples were positive (2-3 nuclei/slide). In the SIM-treated group, the PCNA index was significantly lower than that in the control group ($p\leq0.01$). Additionally, the mean PCNA index was significantly decreased during SIM therapy ($r=-0.61$; $p\leq0.05$) when compared across all analysed time points. The presence of AgNORs in the nuclei from the SIM and Control group are shown in Figs. 6A and 12A, respec-

tively. The mean diameter of the AgNORs was significantly ($p \leq 0.05$) lower in the SIM group compared with the control group. The detailed characteristics of the AgNORs values and immunoreactivities to PCNA, Bcl-2, caspase-3, and mean number of eosinophils are presented in Table 3.

Discussion

Our research demonstrated that SIM negatively affects the liver and causes pronounced changes in hepatocytes, including acute hepatocyte swelling, glycogen depletion, liver hyperaemia, hepatocyte proliferation with occasional pseudoacinar formations, fibrosis, IH, and eosinophil infiltration. SIM also sensitized the hepatocytes to proapoptotic stimuli by decreasing Bcl-2 immunoexpression and enhancing caspase-3 immunoexpression. Additionally, SIM reduced hepatocyte proliferation and transcriptional activity as was reflected in the lower PCNA index and AgNOR diameters.

SIM damaged the hepatocytes by disturbing the cell membrane permeability, as manifested by hepatocellular swelling. Moreover, SIM caused carbohydrate and lipid metabolism distortion, which was reflected by macrovesicular fatty degeneration and diminished glycogen storage. SIM induces oxidative stress, HMG-CoA accumulation and a disturbance of lipid metabolism in the mitochondria (Kaminsky and Kosenko 2010), which may lead to fatty degeneration and necrosis of the hepatocytes with subsequent IH. Reductions of glycogen synthesis after SIM treatment could result from decreased glucokinase activity in the hepatocytes, as verified by others (Musso et al. 2013). Hyperaemia and vein dilatation could be the results of vasodilatory SIM properties. Previous studies have demonstrated that vasodilatation can be connected to the increased production of endothelial nitric oxide synthase (eNOS) caused by SIM. Additionally, statins can reduce the caveolin-1 level; caveolin-1 binds eNOS and thus directly inhibits nitric oxide (NO) production (Plenz et al. 2004). Another explanation could be the activation of the phosphatidylinositol 3-kinase/protein kinase B (Akt) pathway (Simoncini et al. 2000).

In the SIM group, the hepatocyte proliferation with occasional pseudoacinar formation could have been the result of liver regeneration. The regeneration of hepatocytes could be the result of cell damage as evidenced by IH and hepatocyte autoimmune damage by sensitized T lymphocytes. This phenomenon occurs mostly in autoimmune hepatitis (AIH) and drug-induced AIH. Moreover, IH is probably connected to the SIM-mediated inhibition of the HMG-CoA conversion to mevalonate. It has been demonstrated that the continual accumulation of HMG-CoA results in a misbalance of mitochondrial fatty acid and lipid metabolism (Kaminsky and Kosenko 2010). In addition to IH, pseudoacinar formations and fibrosis are also characteristic of AIH (Alla et al. 2006, Christen et al. 2007). Drug-induced AIH can be explained by the elevation of cytochrome P450 (CYP) activity (Christen et al. 2007). Therefore, it should be noted that SIM may cause AIH. SIM also caused a hypersensitivity reaction that was reflected in the increase in the number of eosinophils in the livers. A possible explanation is that SIM caused the induction of STAT6 phosphorylation and the secretion of Th2 cytokines (interleukin (IL)-4, -5 and -10) (Youssef et al. 2002). Additionally, the accumulation of the toxic metabolites of statin may attract eosinophils, and this process is especially prominent in drug-induced liver injury (DILI) (Padda et al. 2011).

We demonstrated that SIM treatment caused decreased Bcl-2 immunoexpression, which indicated the proapoptotic effect of SIM. The present study also demonstrated that on day 19, the Bcl-2 immunoexpression was confined to the periportal hepatocytes and hepatocytes close to the foci of hepatocyte proliferation or fibrotic areas. This pattern suggests that the hepatocytes in these areas execute local defence mechanisms against apoptosis. It has previously been shown that chronic cholestasis during liver cirrhosis can induce Bcl-2 immunoexpression in periportal hepatocytes (Koga et al. 1997). Additionally, the increase in caspase-3 immunoreactivity in the present study may also suggest that SIM has a proapoptotic effect on hepatocytes. Previous studies have demonstrated that SIM can enhance caspases-3, -8, and -9 in hepatocytes due to HMG-CoA inhibition and the subsequent decreases in geranylgeranyl pyrophosphate (GGPP) and Fas-associated death domain (Fas/FADD) system activation (Kubota et al. 2004). The proapoptotic effect of SIM was also confirmed via the TUNEL method.

In our study, SIM treatment reduced PCNA immunoexpression despite the hepatocyte proliferation with the occasional pseudoacinar formation. This phenomenon could be explained by inadequate liver regeneration. The antiproliferative effect of SIM is in agreement with a study on hepatic cancer cells (Relja et al. 2010). The present study demonstrated that the transcriptional activities of the hepatocytes were diminished during SIM administration, and this process was reflected by the lower AgNOR diameters. Therefore, SIM impairs transcriptional activity because transcriptionally active cells exhibit an increase in AgNOR diameter (Underwood 1995).

In conclusion, we demonstrated that SIM administration caused acute hepatocyte swelling, carbohydrate and lipid metabolism distortions, hyperaemia, hepatocyte proliferation with occasional pseudoacinar forma-

tion, IH, fibrosis, and eosinophil infiltration, and these changes are similar to those observed in autoimmune-like DILI. The severity of the morphological alterations increased with the time of SIM administration. Additionally, SIM was demonstrated to have a proapoptotic effect on hepatocytes and to sensitizing them to other proapoptotic factors. Moreover, SIM inhibited hepatocyte proliferation and transcription activity, which was reflected in the reduced liver regeneration capacity. To our knowledge, this is the first study indicating the connection between transcriptional activity and SIM administration. The obtained results make a considerable contribution to the current state of knowledge and may be helpful for determining benefit-risk assessments in SIM therapy.

References

Alla V, Abraham J, Siddiqui J, Raina D, Wu GY, Chalasani NP, Bonkovsky HL (**2006**) Autoimmune hepatitis triggered by statins. J Clin Gastroenterol 40: 757-761.

Armitage J (**2007**) The safety of statins in clinical practice. Lancet 370: 1781-1790.

Bhardwaj SS, Chalasani N (**2007**) Lipid-lowering agents that cause drug-induced hepatotoxicity. Clin Liver Dis 11: 597-613.

Björnsson E, Jacobsen, EI, Kalaitzakis E (**2012**) Hepatotoxicity associated with statins: reports of idiosyncratic liver injury post-marketing. J Hepatol 56: 374-380.

Calderon RM, Cubeddu LX, Goldberg RB, Schiff ER (**2010**) Statins in the Treatment of Dyslipidemia in the Presence of Elevated Liver Aminotransferase Levels: A Therapeutic Dilemma. Mayo Clin Proc 85: 349-356.

Christen U, Holdener M, Hintermann E (**2007**) Animal models for autoimmune hepatitis. Autoimmun Rev 6: 306-311.

Corsini A, Bellosta S, Baetta R, Fumagalli R, Paoletti R, Bernini F (**1999**) New insights into the pharmacodynamic and pharmacokinetic properties of statins. Pharmacol Ther 84: 413-428.

Feulgen R, Rossenbeck H (**1924**) Mikroskopisch-chemischer Nachweis einer Nucleinsäure von Typus der Thymonucleinsäure und auf die darauf beruhende elektive Färbung von Zellkernen in microskopischen Präparaten. Hoppe Seylers Zeitschrift für Physiologische Chemie 135: 203-48.

Huang X, Ma J, Xu J, Su Q, Zhao J (**2015**) Simvastatin induces growth inhibition and apoptosis in HepG2 and Huh7 hepatocellular carcinoma cells via upregulation of Notch1 expression. Mol Med Rep 11: 2334-2340.

Kaminsky YG, Kosenko EA (**2010**) Molecular mechanisms of toxicity of simvastatin, widely used cholesterol-lowering drug. A review. Cent Eur J Med 5: 269-279.

Koga H, Sakisaka S, Ohishi M, Sata M, Tanikawa K (**1997**) Nuclear DNA fragmentation and expression of Bcl-2 in primary biliary cirrhosis. Hepatology 25: 1077-1084.

Kubota T, Fujisaki K, Itoh Y, Yano T, Sendo T, Oishi R (**2004**) Apoptotic injury in cultured human hepatocytes induced by HMG-CoA reductase inhibitors. Biochem Pharmacol 67: 2175-2186.

Lim S, Sakuma I, Quon MJ, Koh KK (**2014**) Differential Metabolic Actions of Specific Statins: Clinical and Therapeutic Considerations. Antioxid Redox Signal 20: 1286-1299.

Macan M, Vukšić A, Žunec S, Konjevoda P, Lovrić J, Kelava M, Štambuk N, Vrkić N, Bradamante V (**2015**) Effects of simvastatin on malondialdehyde level and esterase activity in plasma and tissue of normolipidemic rats. Pharmacol Rep 67: 907-913.

Musso G, Molinaro F, Paschetta E, Gambino R, Cassader M (**2013**) Lipid modifiers and NASH: statins, ezetimibe, fibrates, and other agents. In: Farrell GC, McCullough AJ, Day CP (eds) Non-alcoholic fatty liver disease: a practical guide. Wiley-Blackwell, USA, pp 293-307.

Padda MS, Sanchez M, Akhtar AJ, Boyer JL (**2011**) Drug-induced cholestasis. Hepatology 53: 1377–1387.

Plenz GA, Hofnagel O, Robenek H (**2004**) Differential modulation of caveolin-1 expression in cells of the vasculature by statins. Circulation 109: e7-e8.

Ploton D, Menager M, Jeannesson P, Himber G, Pigeon F, Adnet JJ (**1986**) Improvement in the staining and in the visualization of the argyrophilic proteins of the nucleolar organizer region at the optical level. Histochem J 18: 5-14.

Relja B, Meder F, Wilhelm K, Henrich D, Marzi I, Lehnert M (**2010**) Simvastatin inhibits cell growth and induces apoptosis and G0/G1 cell cycle arrest in hepatic cancer cells. Int J Mol Med 26: 735-741.

Simoncini T, Hafezi-Moghadam A, Brazil DP, Ley K, Chin WW, Liao JK (**2000**) Interaction of oestrogen receptor with the regulatory subunit of phosphatidylinositol-3-OH kinase. Nature 407: 538-541.

Tavintharan S, Ong CN, Jeyaseelan K, Sivakumar M, Lim SC, Sum CF (**2007**) Reduced mitochondrial coenzyme Q10 levels in HepG2 cells treated with high-dose simvastatin: a possible role in statin-induced hepatotoxicity? Toxicol Appl Pharmacol 223: 173-179.

Underwood JC (**1995**) AgNOR measurements as indices of proliferation, ploidy and prognosis. Clin Mol Pathol 48: M239-M240.

Youssef S, Stüve O, Patarroyo JC, Ruiz PJ, Radosevich JL, Hur EM, Bravo M, Mitchell DJ, Sobel RA, Steinman L, Zamvil SS (**2002**) The HMG-CoA reductase inhibitor, atorvastatin, promotes a Th2 bias and reverses paralysis in central nervous system autoimmune disease. Nature 420: 78-84.